Bulletin of Electrical Engineering and Informatics
Vol. 15, No. 2, April 2026, pp. 1082∼1095
ISSN: 2302-9285, DOI: 10.11591/eei.v15i2.10284

An efficient spectrum sensing method using convolutional neural network and filter banks for cognitive radio

Hamza Ouamna, Noureddine El-Haryqy, Anass Kharbouche, Zhour Madini, Younes Zouine
Laboratory of Advanced Systems Engineering (ISA), Department of Electrical and Telecommunication, National School of Applied Sciences (ENSA), Ibn Tofail University, Kenitra, Morocco

Article Info

Article history:

Received Mar 16, 2025
Revised Feb 7, 2026
Accepted Mar 10, 2026

Keywords:

Cognitive radio
Deep learning
Energy level detection
FB-CNN
Filter bank detection
Spectrum sensing

ABSTRACT

The rapid advancement of connected vehicle technologies has intensified the need for efficient spectrum utilization. Cognitive radio (CR) enables dynamic access to underutilized spectrum, with spectrum sensing playing a key role in detecting primary users (PU). This study introduces a novel spectrum sensing approach that integrates filter bank (FB) signal decomposition with convolutional neural networks (CNNs)—referred to as filter bank decomposition and convolutional neural network (FB-CNN)—to enhance detection performance compared to conventional methods. Unlike traditional techniques such as energy detection (ED), the proposed FB-CNN leverages the frequency components extracted by the FB as CNN inputs, enabling robust identification of PU signals across multiple modulation schemes, including BPSK, QAM, FSK, and GMSK. Simulation results demonstrate substantial gains, particularly in low-SNR scenarios: for example, at an SNR of 5 dB, FB-CNN achieves a detection probability of 89% for 2-FSK, compared to only 22% with ED—representing a fourfold improvement. These findings highlight the novelty and effectiveness of FB-CNN in significantly improving spectrum sensing reliability for connected vehicle networks operating in challenging signal environments.

This is an open access article under the CC BY-SA license.

Corresponding Author:

Hamza Ouamna
Laboratory of Advanced Systems Engineering (ISA), Department of Electrical and Telecommunication
National School of Applied Sciences (ENSA), Ibn Tofail University
Kenitra, 14000, Morocco
Email: hamza.ouamna@uit.ac.ma

1. INTRODUCTION

The rapid evolution of intelligent transportation systems has accelerated the adoption of advanced technologies such as autonomous driving, LiDAR, radar, and connected vehicle communication. Among these, vehicular connectivity—encompassing vehicle-to-vehicle (V2V), vehicle-to-infrastructure (V2I), and vehicle-to-pedestrian (V2P) links—has attracted particular attention for its potential to enhance road safety, traffic efficiency, and infotainment services [1], [2]. To facilitate these applications, the Federal Communications Commission (FCC) allocated 75 MHz of spectrum in the 5.9 GHz band for wireless access in vehicular environments (WAVE). However, the coexistence of safety-critical communication and high-data-rate services has intensified spectrum scarcity, highlighting the limitations of static spectrum allocation where some frequency bands are congested while others remain underutilized. Dynamic spectrum access (DSA) via cognitive radio (CR) has emerged as a promising paradigm to overcome this limitation. CR enables secondary users to opportunistically access underutilized frequency bands without causing harmful interference to primary users

(PU) [3], [4]. Central to this functionality is spectrum sensing, which continuously monitors the radio environment to detect spectrum availability while minimizing false alarms and missed detections [5]–[7]. Several classical spectrum sensing techniques have been investigated. Energy detection (ED) is computationally efficient but suffers from noise uncertainty. Matched filtering (MF) provides optimal detection when the PU's signal is known, a condition rarely satisfied in dynamic vehicular environments. Feature detection (FD) can achieve good performance at low signal-to-noise ratios (SNRs) but requires significant computational resources [8]–[10]. More recently, machine learning and deep learning methods have been introduced to enhance sensing robustness; however, most of these rely on raw time-domain data or handcrafted features, which limits their ability to generalize across diverse modulation types and noisy environments.

Despite these advancements, important challenges remain unresolved. Reliable detection accuracy under low-SNR and noisy conditions is still difficult to achieve, particularly in safety-critical vehicular environments. Existing methods also struggle to adapt to multiple modulation formats without prior knowledge of the signal, while high computational demands limit their practicality for real-time applications. These challenges underline the need for a spectrum sensing approach that is both accurate and robust, while also being computationally feasible. To address these limitations, we propose a novel spectrum sensing framework based on filter bank decomposition and convolutional neural networks (FB-CNN). In the proposed approach, a filter bank (FB) decomposes the received signal into multiple subbands, preserving fine-grained spectral details, while the CNN automatically learns discriminative patterns across these subbands to distinguish between occupied and vacant channels. Unlike conventional CNN-based methods that process raw signals directly, our approach leverages multi-band frequency-domain features, enhancing robustness to noise and improving generalization across various modulation types such as BPSK, QAM, FSK, and GMSK. Furthermore, a dynamic thresholding mechanism stabilizes the probability of detection under varying noise conditions, effectively reducing false alarm rates [11]–[13]. Through extensive simulations, we demonstrate that FB-CNN outperforms traditional methods in terms of detection probability, noise resilience, and adaptability to different modulation schemes. The remainder of this paper is organized as follows. Section 2 reviews related work on spectrum sensing techniques. Section 3 presents the system model, describes the proposed FB-CNN framework in detail and analyzes the simulation results. Section 4 presents the results and provides a detailed discussion of the findings. Finally, section 5 concludes the paper and highlights potential directions for future research.

2. RELATED WORK

The concept of spectrum sensing has evolved significantly with the emergence of machine learning and deep learning techniques, particularly CNN. Traditional methods such as ED, FB-based sensing, and cyclostationary FD have been widely used for spectrum sensing. However, these approaches often suffer from high false alarm rates and poor performance in low SNR environments. Recent advancements in deep learning have introduced CNN-based techniques that enhance spectrum sensing accuracy and robustness [14], [15]. Ding *et al.* [16] introduced a FB-CNN to classify short-time steady-state visual evoked potential (SSVEP) signals. Their model utilizes FBs to preprocess signals before passing them through CNN layers, significantly improving classification performance. Similarly, Xu *et al.* [17] extended this approach by proposing a filter bank complex spectrum convolutional neural network (FB-CCNN) for SSVEP classification. Their method leverages the complex spectrum of the signals and demonstrates superior accuracy in brain-computer interface applications. For CR networks, Zhang *et al.* [18] explored a novel multiband spectrum sensing technique using a covariance matrix-aware CNN. Their approach integrates the sample covariance matrix of received signals as input to a CNN model, leading to improved detection performance across multiple frequency bands. This technique is particularly effective in DSA scenarios, where the spectral environment changes frequently. Additionally, Novelo and Dolecek [19] investigated the use of filter banks (FBs) in CNNs for texture classification tasks. Their findings indicate that incorporating FBs into CNN architectures enhances feature extraction capabilities, making them well-suited for tasks requiring fine-grained spectral analysis. This work serves as a foundation for applying similar methodologies in spectrum sensing applications. Bassi and Attux [20] introduced the FBDNN model, which integrates FBs with deep neural networks to improve SSVEP classification. Their work focuses on portable and fast brain-computer interfaces, demonstrating that FB techniques can effectively enhance signal classification performance while maintaining computational efficiency. Building on these advancements, the method proposed in this work extends the application of FB-based CNN architectures for spectrum sensing, introducing a novel approach that improves detection accuracy in low-SNR environments.

3. MATERIAL AND METHODS

3.1. Energy level detection

Energy level detection is one of the simplest and most resource-efficient techniques for spectrum sensing [21]. This method is widely used because it does not require prior knowledge of the signal's structure, making it suitable for a variety of communication scenarios. The core idea is to measure the total energy present in a frequency band and compare it with a predefined threshold to determine whether the channel is occupied. The process begins by transforming the received signal from the time domain to the frequency domain using a fast Fourier transform (FFT). This transformation allows the system to analyze the frequency components of the signal, which is essential for detecting occupied channels. After the FFT, the vehicle estimates the power spectral density (PSD) of the signal using (1):

$$\text{PSD}(f) = \lim_{T\to\infty} \frac{1}{T} \left| \sum_{n=0}^{T-1} x[n] e^{-j2\pi f n} \right|^2 \tag{1}$$

In this equation, $x[n]$ represents the sampled signal in the time domain, f is the frequency, and T is the number of samples. The PSD essentially provides a measure of how the signal's power is distributed over different frequencies. Once the PSD is obtained, the total energy in the frequency band can be calculated as (2):

$$E = \sum_{f} \text{PSD}(f) \tag{2}$$

The computed energy E is then compared to a predefined threshold γ. If the measured energy exceeds γ, the system concludes that the channel is occupied; otherwise, it is deemed free for transmission. This decision-making process enables the vehicle to dynamically select the most suitable channel for communication, thereby improving overall spectral efficiency [22], [23]. Figure 1 presents an example of the noise variance profile used in the detection simulation. In this scenario, an ED threshold of 3 dBm was chosen, corresponding to a 2% false alarm probability. This means that in 2% of cases, the system might incorrectly classify an unoccupied channel as occupied purely due to noise fluctuations.

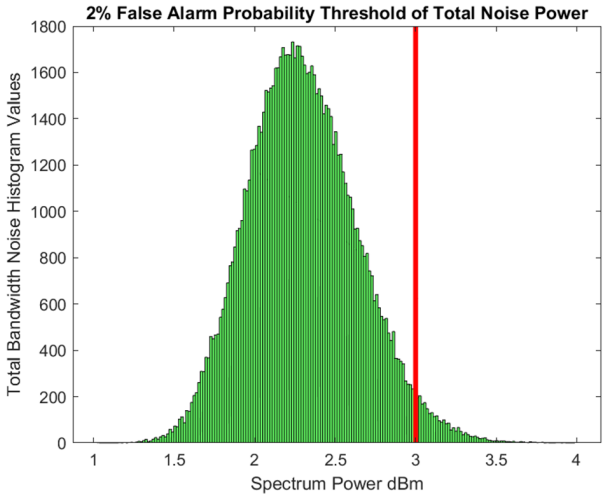

Figure 1. 2% false alarm probability threshold of total noise power

When a signal is introduced into the system, the underlying Gaussian noise distribution—originally centered around the noise floor—shifts toward higher energy values. As this shift occurs, a greater proportion of the distribution surpasses the detection threshold, thereby increasing the likelihood of correctly identifying the presence of the signal. From a statistical perspective, this modification alters the overlap between the noise-only and signal-plus-noise probability density functions, leading to changes in the detection metrics. When plotted as the probability of detection versus SNR, the resulting curve often exhibits an S-shaped form, reflecting a

gradual transition from low to high detection probability. This behavior, which will be explored in more detail in section 4 demonstrates how the system's detection capability systematically improves as the signal power rises relative to the noise level, ultimately reducing the probability of missed detections.

3.2. Filter bank-based detection

FB-based spectrum sensing detects the presence of signals by decomposing the received signal into multiple subbands using a set of band-pass filters. Unlike methods that rely on a known reference waveform, this approach is particularly effective in environments contaminated by additive white Gaussian noise or uncorrelated interference, as it enhances signal separation and mitigates noise effects. The core principle involves splitting the received signal into multiple frequency subbands through a bank of filters, typically implemented via polyphase decomposition, where each filter extracts a specific frequency component for independent ED. By analyzing energy levels in different frequency bins, the system determines whether a PU is active or inactive. The received signal is first passed through band-pass filters corresponding to different frequency subbands, the energy in each subband is estimated, and a decision threshold is applied to detect potential spectrum occupancy based on whether the detected energy exceeds the threshold. Figure 2 presents the block diagram of the FB processing.

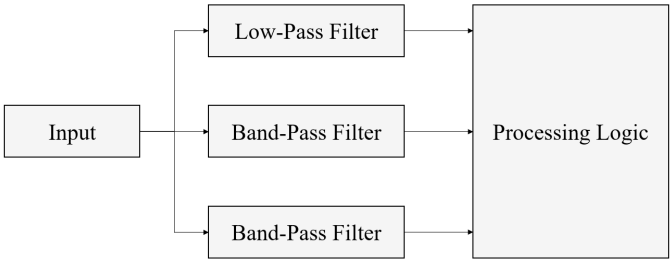

Figure 2. Block diagram of the FB processing

3.3. Filter bank design

For this application, our filter design does not prioritize synthesis bank or perfect reconstruction conditions in the synthesis bank domain. The primary focus is on achieving a FB with low stop-band rejection, ensuring that out-of-band noise power remains minimal. Additionally, phase distortion in the FB design should be kept to significantly low dB values (below 60 dB) to prevent any decoherence that could interfere with detection [24], [25]. A simple M-point DFT-based FB was constructed with M=3, with the choice of three bands being arbitrarily selected to demonstrate the impact of proper filtering on spectrum sensing. For the transmit channel, the normalized frequency bands were sufficient to align the transmission bandwidth with one of the channel frequency lengths (MF). In real-world applications, the number of channels could be much higher [26], [27]. Figure 3 shows the frequency response of the FB in Simulink.

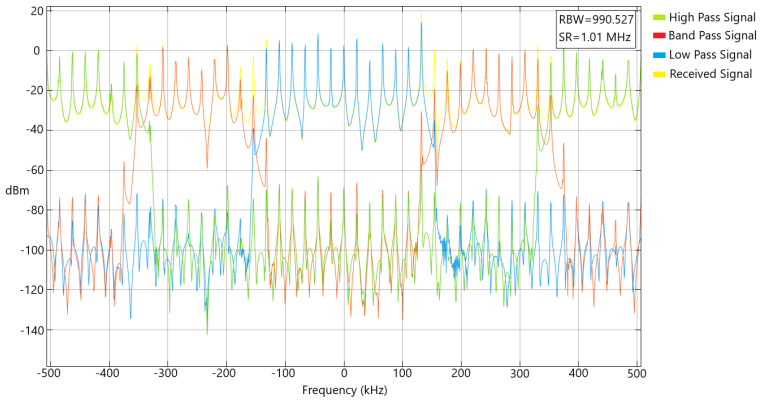

Figure 3. Magnitude response of FB

3.4. Implementation

To perform an analysis of FB based detection and FB CNN-based detection, a Simulink-based signal generation system (shown in Figure 4) was created to generate data. This system consists of a BPSK, GMSK, 2-FSK, 4-FSK, 16-QAM, and 32-QAM modulated signal, transmitting at baseband and up-sampled by a factor of 4. Both the up-sampling and pulse shaping occur in the "Square root" filter block, where the sampling factor and root-raised cosine filter are applied. The transmitted signal is then amplified and combined with a "Random Source" block, which introduces a Gaussian noise floor (as shown in Figure 3). The system transmits and receives at 200 samples per frame, and after 100 seconds of simulation, it produces 120 Mb of IQ data. This general approach is highly effective for generating data at the physical layer [28].

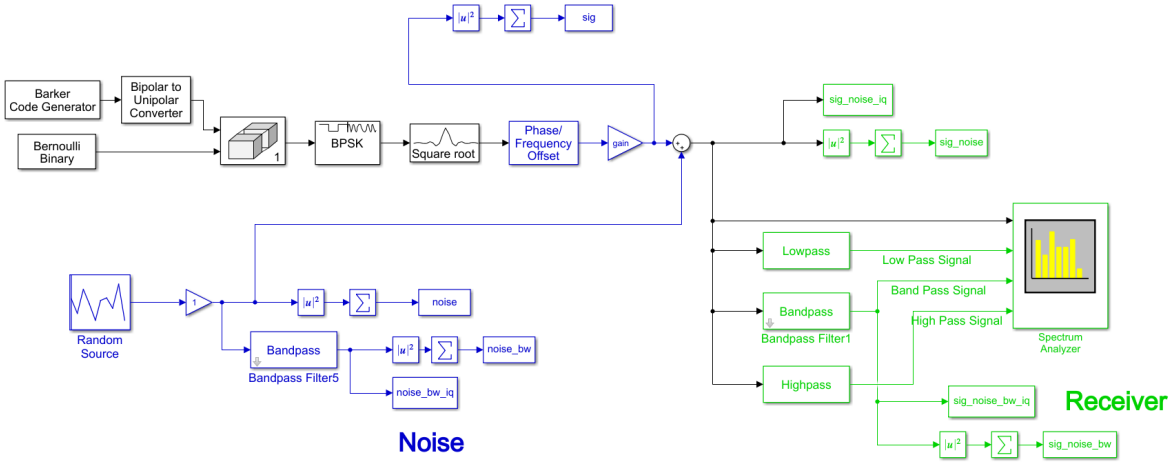

Figure 4. Implementation of FB method using Simulink for BPSK

3.5. Received signal model

The received baseband signal at the secondary user (SU) can be expressed as (3):

$$r(t) = \begin{cases} s(t) + n(t), & H_1 \quad \text{(PU present)} \\ n(t), & H_0 \quad \text{(PU absent)} \end{cases} \tag{3}$$

where H_1 represents the hypothesis that the spectrum is occupied, H_0 represents the hypothesis that the spectrum is idle, $s(t)$ is the transmitted PU signal, and $n(t) \sim \mathcal{CN}(0, \sigma_n^2)$ is complex Gaussian noise.
In discrete time, this becomes:

$$r[n] = \begin{cases} s[n] + n[n], & H_1 \\ n[n], & H_0 \end{cases} \tag{4}$$

The received signal consists of in-phase (I) and quadrature (Q) components:

$$r[n] = I[n] + jQ[n] \tag{5}$$

Which is processed by a FB to decompose it into frequency subbands.

3.6. Filter bank-based subband decomposition

The received IQ signal is passed through a quadrature mirror filter bank (QMFB) to split it into multiple frequency subbands:

$$r_k[n] = \sum_m r[m] h_k[n-m], \quad k = 1, 2, \ldots, K \tag{6}$$

where K is the number of subbands and $h_k[n]$ is the impulse response of the k-th subband filter.

The frequency response of each filter satisfies:

$$\sum_{k=1}^{K} H_k(f) \approx 1, \quad \forall f \tag{7}$$

Each subband signal retains both IQ components:

$$r_k[n] = I_k[n] + jQ_k[n] \tag{8}$$

3.7. Convolutional neural network mathematical model

In the following, we present the mathematical formulation of the proposed CNN model. The model is designed to process raw in-phase (I) and quadrature (Q) components of the received signal, extracting relevant features to determine whether the spectrum is occupied or idle. The architecture leverages convolutional layers to capture local dependencies in the IQ data, followed by fully connected layers for classification.

3.7.1. Input representation

The input to the model is represented as a real-valued matrix:

$$\mathbf{X} \in \mathbb{R}^{1024\times 2} \tag{9}$$

where 1024 denotes the number of time-domain samples in each input instance. This corresponds to a temporal window over which the model is trained and 2 represents I and Q components.

The received signal, initially in the form of a complex-valued sequence $s[n] = I[n] + jQ[n]$, is transformed into the real-valued matrix X by separating the real and imaginary parts into two distinct columns. This transformation enables direct processing by the CNN while preserving the temporal structure of the signal.

3.7.2. Convolutional neural network architecture

Table 1 summarizes the proposed neural network architecture [29], [30]. The convolutional layers in the CNN apply one-dimensional convolutions to extract temporal dependencies from the input IQ data. Each convolution operation at layer l for the k-th filter is mathematically defined as (10):

$$F_k^{(l)}[n] = f\left(\sum_m W_k^{(l)}[m] \cdot X^{(l)}[n-m] + b_k^{(l)}\right) \tag{10}$$

where $W_k^{(l)}$ represents the learnable convolutional filter weights at layer l for the k-th filter, and $b_k^{(l)}$ is the corresponding bias term. The activation function $f(\cdot)$ introduces non-linearity to enhance the model's learning capacity. In this case, the rectified linear unit (ReLU) activation function is applied:

$$f(x) = \max(0, x) \tag{11}$$

which ensures that only positive activations are propagated, mitigating the vanishing gradient problem and improving the model's efficiency. Following the convolutional layers, pooling layers are introduced to reduce the temporal resolution of the extracted feature maps while preserving essential information. Max-pooling is used, which selects the maximum value within a sliding window of size S, and is defined as (12):

$$X_{\text{pool}}^{(l)}[n] = \max_{m\in[0,S-1]} X^{(l)}[nS+m] \tag{12}$$

where S is the stride size. Pooling reduces the dimensionality of the feature maps, leading to lower computational complexity and helping prevent overfitting. After feature extraction, the pooled feature maps are flattened and passed through fully connected layers to perform classification. This transformation is represented as (13):

$$\mathbf{y} = \text{softmax}(W_{\text{fc}} X_{\text{pooled}} + b_{\text{fc}}) \tag{13}$$

where W_{fc} and b_{fc} are the weights and biases of the fully connected layer, and $\text{softmax}(\cdot)$ converts the output into a probability distribution over the possible classes:

$$\mathbf{y} = [P(H_0), P(H_1)] \tag{14}$$

where $P(H_0)$ denotes the probability that the spectrum is idle, and $P(H_1)$ represents the probability that the spectrum is occupied. The final classification decision is made by comparing $P(H_1)$ against a predefined decision threshold λ. The spectrum sensing decision rule is expressed as (15):

$$\hat{H} = \begin{cases} H_1, & P(H_1) > \lambda \\ H_0, & \text{otherwise} \end{cases} \tag{15}$$

where $\hat{H}$ is the estimated hypothesis, with H_1 indicating an occupied spectrum and H_0 indicating an idle spectrum. The threshold λ can be adjusted to balance detection performance and false alarm rates, enabling adaptive spectrum sensing in dynamic wireless environments.

Table 1. Neural network architecture of the proposed FB-CNN model used for spectrum sensing

Index	Layers	Output dimension
1	Input layer	1024×2
2	1×16 convolution (128 filters)	1024×2
3	Batch normalization	1024×2
4	ReLU activation	1024×2
5	MaxPooling (1×2, Stride 1×2)	512×2
6	1×16 convolution (64 filters)	512×2
7	Batch normalization	512×2
8	ReLU activation	512×2
9	MaxPooling (1×2, Stride 1×2)	256×2
10	1×16 convolution (32 filters)	256×2
11	Batch normalization	256×2
12	ReLU activation	256×2
13	AveragePooling (1×8)	32×2
14	Fully connected layer (20 neurons)	20×1
15	Fully connected layer (10 neurons)	10×1
16	Fully connected layer (2 neurons)	2×1
17	Softmax layer	2×1
18	Classification output	2×1

3.7.3. Justification of convolutional neural networks architecture

The architecture was designed with three convolutional layers to capture features at different abstraction levels while avoiding over-parameterization. The first convolutional layer (128 filters, kernel size 1×16) extracts short-term temporal dependencies in the IQ data, where the kernel length of 16 corresponds approximately to the symbol duration of many digital modulation formats. This makes the layer particularly effective at detecting modulation-specific transitions and noise patterns. The second and third convolutional layers progressively reduce the number of filters (64 and 32). This funnel-shaped design compresses the feature space, forcing the network to retain only the most discriminative patterns. The second layer captures mid-level features such as spectral harmonics and subband energy distributions, while the third layer learns global features that are robust to SNR variations and channel noise. Pooling layers were chosen deliberately: max-pooling preserves dominant features by selecting the strongest activation within each window, whereas average pooling before the fully connected layers smooths representations and mitigates overfitting. The fully connected layers (20–10–2 neurons) gradually reduce dimensionality, allowing the network to combine low- and high-level features into compact decision boundaries for binary classification. This progressive reduction ensures better generalization while keeping computational cost low. Thus, each design choice—kernel size, number of layers, filter progression, and pooling type—was selected to balance detection accuracy, generalization across modulation formats, and computational efficiency for real-time spectrum sensing in vehicular environments.

3.8. Training process

The training process was performed on an Intel Core i5 11th generation processor, which provides sufficient computational capacity for prototyping but imposes constraints on large-scale training. All network parameters were randomly initialized using a Gaussian distribution. The mini-batch size was set to 128, and the stochastic gradient descent (SGD) method with momentum was employed, using a momentum factor of 0.9. The initial learning rate was set to 0.02, and every 3 epochs the learning rate was reduced by a factor of 10. The model was trained over 10 epochs, with validation performed every 500 iterations. The decision

to limit training to 10 epochs was based on empirical validation: additional epochs did not yield significant improvements in detection probability and, in some cases, led to early signs of overfitting. This suggests that the model converges rapidly under the chosen optimization strategy. Nonetheless, for broader generalization across different noise models and unseen modulation formats, extended training or statistical analysis across multiple independent runs would further strengthen reliability. Algorithm 1 outlines the training loop, which includes pre-processing steps, weight updates using SGD with momentum, dynamic learning rate adjustments, and integrated validation/testing to monitor model performance throughout the process. While the current setup demonstrates proof-of-concept feasibility, hardware-accelerated platforms such as GPUs or TPUs would enable deeper models, longer training cycles, and larger datasets, thereby improving scalability and robustness for real-world deployment. Future work will explore these extensions to enhance generalization and efficiency.

Algorithm 1. Training process

Pre-processing:
Split the raw signal data into fixed-length time frames
Normalize the signal samples
Initialize the CNN Model:
Initialize the weights and biases
Training Loop:
Set mini-batch size to 128
Set momentum factor to 0.9
Set initial learning rate to 0.02

for each epoch (maximum 10 epochs) **do**
    Shuffle the training data to avoid bias

    for each training sample in the mini-batch **do**
        Feed the input sequence into the CNN
        Update the weights and biases using SGD with momentum
    end for
    if epoch mod 3 = 0 **then**
        Reduce learning rate by a factor of 1/10
    end if
    Validation:
    Perform validation every 500 iterations
    Calculate performance metrics
end for
Testing:
Pre-process the test signal data
Feed the input sequence into the trained model
Get the predicted output from the model

4. RESULTS AND DISCUSSION

4.1. Metrics for performance evaluation

To evaluate the classification performance of our model, we use the probability of detection (P_d) as a key metric. The probability of detection is employed in signal processing and machine learning to assess a classifier's ability to correctly identify the presence of a signal in a noisy environment. It is defined as (16):

$$P_d = P(\hat{H}_1|H_1) \tag{16}$$

where $\hat{H}_1$ represents the decision that a signal is present and H_1 denotes the actual presence of the signal.

We select this metric because it provides a comprehensive evaluation of the model's performance across different SNR levels. By varying the SNR, we can simulate different noise conditions and analyze the model's robustness under diverse scenarios. Additionally, using P_d allows for direct comparisons with other

models and traditional approaches, enabling a more thorough performance assessment and helping to identify areas for improvement.

4.2. System threshold definition

The noise floor variance in our system follows the normal distribution, as illustrated in Figure 5. To take advantage of this property, we will extract the threshold for bandwidth spectrum for a desired probability of detection. The threshold is a critical parameter in determining the performance of our system, as it determines the sensitivity of the detector. By extracting the threshold from the normal distribution, we can determine the point at which a signal will be detected with a high probability. This allows us to set a desired level of performance for our system and ensures that we are able to detect signals of interest while minimizing false alarms. Furthermore, by extracting the threshold for the total spectrum and bandwidth, we can optimize the performance of our system for different signal types and noise environments. This approach allows us to achieve the best possible performance for our system and is a common method used in signal processing and telecommunications systems.

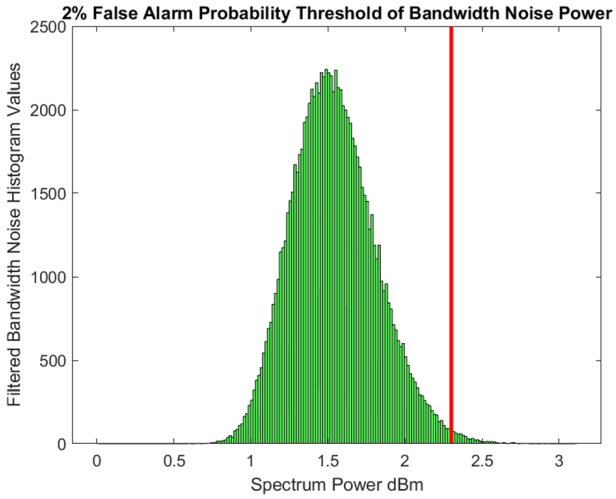

Figure 5. 2% false alarm probability threshold of bandwidth noise power

The neural network defined in Table 1 has been trained with the Adam optimizer. The Adam optimizer is a popular algorithm for training neural networks because it combines the advantages of both gradient descent and momentum-based optimization. It is computationally efficient and has been shown to converge quickly to a good solution. We have used categorical cross-entropy as the loss function. The categorical cross-entropy is an appropriate loss function for this problem because it measures the dissimilarity between the predicted and true categorical probability distributions. To ensure that the model generalizes well, we divided the IQ dataset into 70% for training instances and 30% for validation instances. This allows us to evaluate the model's performance on unseen data and make adjustments to the model if necessary. This division of the dataset also allows us to monitor the overfitting, which is common in neural network models.

To measure the performance of our model, we have plotted the probability of detection versus SNR predicted by the neural network. This allows us to evaluate the ability of the model to correctly identify the presence of a signal in a noisy environment. We have also plotted the probability of detection versus SNR predicted using the energy level method. This is a traditional method used in signal processing to evaluate the performance of a classifier. By comparing the performance of the neural network and the energy level method, we can gain insight into the effectiveness of our model and identify areas for improvement. The figures show the plots for the two methods, which allow us to compare them visually and understand the performance of our model, this way we can have a better understanding of our model and evaluate if it is suitable for our application

4.3. Experimental results

In this section, we evaluate the detection performance of the proposed FB-based CNN spectrum sensing technique in comparison with the conventional energy detector. The probability of detection (P_d) is ana-

lyzed as a function of the SNR for various modulation schemes, including 2-FSK, 4-FSK, 16-QAM, 32-QAM, BPSK, and GMSK. The results, summarized in Figure 6, consistently show that the proposed deep learning-based method achieves substantially higher detection probabilities, particularly under low-SNR conditions.

We found that P_d correlates strongly with the modulation complexity and SNR level, with the FB-CNN achieving disproportionately higher detection rates in challenging noise conditions. For example, in 2-FSK (Figure 6(a)), the proposed method achieves approximately 89% P_d at -5 dB SNR, compared to only 22% for the energy detector. Similarly, for 4-FSK (Figure 6(b)), P_d reaches 95% at 0 dB with FB-CNN, versus 40% with the traditional approach.

For higher-order modulations such as 16-QAM (Figure 6(c)) and 32-QAM (Figure 6(d)), the proposed method achieves P_d values of 96% and 97% at 5 dB and 7 dB SNR, respectively—more than double the performance of the energy detector in these cases. Lower-order modulations also benefit greatly: for BPSK (Figure 6(e)), P_d is 93% at -5 dB with FB-CNN, compared to 30% with ED; for GMSK (Figure 6(f)), P_d exceeds 94% at -3 dB, versus only 35% for the baseline.

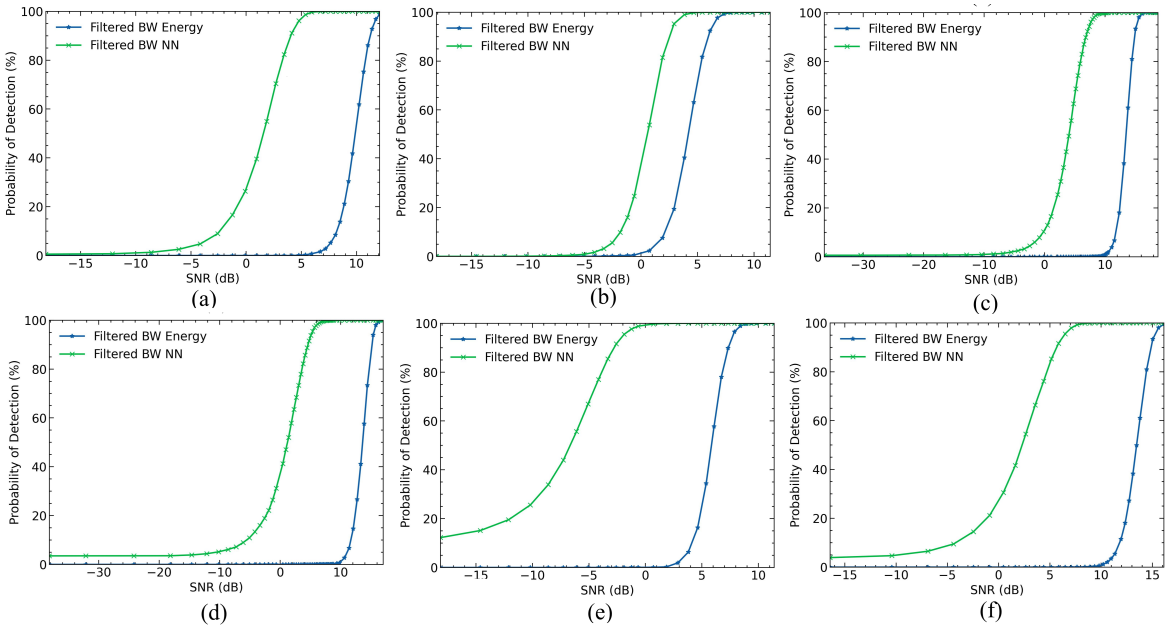

Figure 6. Detection probability (P_d) comparison between the proposed FB-CNN and conventional energy detector for different modulation schemes: (a) 2-FSK, (b) 4-FSK, (c) 16-QAM, (d) 32-QAM, (e) BPSK, and (f) GMSK

Our findings indicate that higher modulation complexity is not associated with poor detection performance when using the FB-CNN approach, in contrast to what has been observed in conventional spectrum sensing studies [8], [9]. The proposed method benefits from FB decomposition, which preserves frequency-domain features across subbands, and deep CNN classification, which enhances resilience to noise uncertainty—without negatively affecting adaptability to diverse modulation schemes. This aligns with recent work in [11], [12], which also emphasized the role of learned spectral features in improving detection at low SNR, but our results extend these insights to a broader set of modulations and operating conditions.

Table 2 summarizes the detection performance of the proposed FB-CNN and the conventional energy detector at an SNR of 4 dB for different modulation schemes. The energy detector shows very poor performance, achieving 0% detection for several modulations and only 44.92% for 4-FSK. In contrast, the FB-CNN achieves significantly higher detection probabilities, reaching 100% for BPSK and 99.15% for 4-FSK, while maintaining strong performance across other modulations. Overall, these results highlight that the proposed FB-CNN framework delivers consistently high detection probabilities across modulation types and SNR levels, confirming its potential for real-world DSA in connected vehicular and other CR networks.

Table 2. (P_d) comparison between the proposed FB-CNN and conventional energy detector at SNR=4 dB

Modulation	2-FSK (%)	4-FSK (%)	16-QAM (%)	32-QAM (%)	BPSK (%)	GMSK (%)
Energy detector	0	44.92	0	0	8.75	0
FB-CNN	89.39	99.15	49.59	84.64	100	71.5

4.4. Comparison with prior work

To provide a fair benchmark, we compared our proposed FB-CNN model with results reported in prior work on deep learning–based spectrum sensing. In particular, [31] evaluated several classifiers, including support vector machine (SVM), logistic regression (LR), convolutional neural network (CNN), long short-term memory (LSTM), and a hybrid LSTM-CNN model. At an operating point of SNR = 4 dB, interpolation from their published results shows that LSTM-CNN achieves the highest probability of detection (95%), followed by LSTM (93%) and CNN (90%). In contrast, classical approaches such as SVM and LR lag slightly behind with 88% and 89% detection probability, respectively. Table 3 summarizes these results. This comparison highlights that while our FB-CNN model achieves competitive performance under noisy conditions, hybrid temporal–convolutional architectures can offer additional gains in temporal pattern recognition tasks, suggesting a promising direction for future extensions.

Table 3. Interpolated performance of different deep learning models at SNR=4 dB, adapted from [31]

Model	Pd @ 4 dB (%)
SVM	88
LR	89
CNN	90
LSTM	93
LSTM-CNN	95

4.5. Limitation of the proposed method

This study investigated a comprehensive spectrum sensing framework combining FB signal decomposition with CNN, demonstrating resilience in low-SNR and noisy conditions. However, additional and in-depth research may be required to confirm its scalability and adaptability, particularly in highly dynamic vehicular communication environments where spectrum occupancy changes rapidly. While the computational complexity has been optimized compared to conventional deep learning approaches, the proposed method still requires efficient hardware implementations—such as FPGA or ASIC solutions—for real-time deployment in resource-constrained devices. This limitation may impact the system's practicality in large-scale vehicular networks if not addressed. Another limitation concerns the method's performance under channel fading and multipath propagation. Since the current evaluation is primarily under AWGN conditions, the robustness of feature extraction in fading-dominated channels remains uncertain. Future studies should explicitly address these propagation impairments to ensure reliability in realistic environments. In addition, latency trade-offs in real-time demodulation must be considered. Although the FB-CNN design is more lightweight than conventional deep learning architectures, the convolutional and fully connected layers still introduce non-negligible inference delays. In mission-critical spectrum access scenarios, these delays could hinder timely decision-making, making optimizations such as pruning, quantization, or deployment on hardware accelerators necessary.

The framework also shows sensitivity to parameter selection, particularly in the FB design and CNN hyperparameters (e.g., kernel sizes, pooling strategies, and learning rate schedules). Small deviations can lead to noticeable performance variations, which suggests a need for systematic tuning or automated optimization approaches to achieve consistent results across different deployment scenarios. Furthermore, although the model exhibits strong generalization to multiple modulation formats, its performance across a broader set of frequency bands, modulation schemes, and non-line-of-sight conditions has yet to be fully validated. Our results indicate that FB-CNN is more resilient to noise uncertainty than traditional spectrum sensing methods. Future research may explore lightweight neural network architectures that reduce inference time while preserving detection accuracy, as well as adaptive learning strategies enabling the model to retrain on-the-fly in response to evolving spectrum conditions. Practical investigations into real-world vehicular testbeds, diverse geographic regions, and spectrum sharing scenarios with heterogeneous communication systems will be essential to ensure robustness, scalability, and regulatory compliance.

5. CONCLUSION

This work has presented a novel spectrum sensing framework that integrates FB signal decomposition with CNNs for PU detection in connected vehicle networks. The proposed FB-CNN approach achieves: i) improved accuracy, with detection probability gains of 5–10 dB over conventional ED, and up to a fourfold improvement for certain modulation schemes in low-SNR conditions; ii) enhanced robustness, owing to FB-based spectral feature extraction that mitigates noise sensitivity; and iii) broad applicability, with support for multiple modulation formats (BPSK, QAM, FSK, and GMSK) and adaptability through dynamic thresholding. While the results demonstrate clear advantages, the study is limited to simulated environments and a predefined set of modulation schemes. Performance under complex real-world conditions—such as multipath fading, shadowing, and interference from non-cooperative sources—remains to be validated. Furthermore, the computational cost of CNN inference may impact deployment on resource-constrained platforms. Future work will address these limitations by conducting field trials in vehicular and roadside units, investigating higher-order modulation schemes, and developing adaptive or online learning mechanisms for dynamic spectrum environments. Additionally, lightweight neural architectures and model compression techniques will be explored to reduce latency and power consumption for embedded automotive applications.

FUNDING INFORMATION

No funding has been provided for this study.

AUTHOR CONTRIBUTIONS STATEMENT

This journal uses the Contributor Roles Taxonomy (CRediT) to recognize individual author contributions, reduce authorship disputes, and facilitate collaboration.

Name of Author	C	M	So	Va	Fo	I	R	D	O	E	Vi	Su	P	Fu
Hamza Ouamna	✓	✓	✓	✓	✓	✓		✓	✓	✓			✓	
Noureddine El-Haryqy		✓	✓	✓		✓			✓	✓				
Anass Kharbouche		✓				✓		✓	✓	✓	✓	✓		
Zhour Madini	✓				✓					✓		✓	✓	
Younes Zouine	✓				✓					✓		✓	✓	

C : **C**onceptualization
M : **M**ethodology
So : **So**ftware
Va : **Va**lidation
Fo : **Fo**rmal Analysis
I : **I**nvestigation
R : **R**esources
D : **D**ata Curation
O : Writing - **O**riginal Draft
E : Writing - Review & **E**diting
Vi : **Vi**sualization
Su : **Su**pervision
P : **P**roject Administration
Fu : **Fu**nding Acquisition

CONFLICT OF INTEREST STATEMENT

The authors declare that they have no known competing financial interests or personal relationships that could have appeared to influence the work reported in this paper.

DATA AVAILABILITY

The data that support the findings of this study are available upon request from the corresponding author.

REFERENCES

[1] H. Ouamna, A. Kharbouche, N. El-Haryqy, Z. Madini, and Y. Zouine, "Performance analysis of a hybrid complex-valued CNN-TCN model for automatic modulation recognition in wireless communication systems," *Applied System Innovation*, vol. 8, no. 4, p. 90, 2025, doi: 10.3390/asi8040090.

[2] S. N. Syed *et al.*, "Deep Neural Networks for Spectrum Sensing: A Review," *IEEE Access*, vol. 11, pp. 89591-89615, 2023, doi: 10.1109/ACCESS.2023.3305388.

[3] M. Hao, H. Li, G. Xu, S. Liu, and H. Yang, "Towards Efficient and Privacy-Preserving Federated Deep Learning," in *ICC 2019 - 2019 IEEE International Conference on Communications (ICC)*, Shanghai, China, 2019, pp. 1-6, doi: 10.1109/ICC.2019.8761267.

[4] L. Cai, K. Cao, Y. Wu, and Y. Zhou, "Spectrum Sensing Based on Spectrogram-Aware CNN for Cognitive Radio Network," *IEEE Wireless Communications Letters*, vol. 11, no. 10, pp. 2135-2139, Oct. 2022, doi: 10.1109/LWC.2022.3194735.

[5] S. Solanki, V. Dehalwar, J. Choudhary, M. L. Kolhe, and K. Ogura, "Spectrum Sensing in Cognitive Radio Using CNN-RNN and Transfer Learning," *IEEE Access*, vol. 10, pp. 113482-113492, 2022, doi: 10.1109/ACCESS.2022.3216877.

[6] L. Li, W. Xie, and X. Zhou, "Cooperative Spectrum Sensing Based on LSTM-CNN Combination Network in Cognitive Radio System," *IEEE Access*, vol. 11, pp. 87615-87625, 2023, doi: 10.1109/ACCESS.2023.3305483.

[7] D. Chew and A. B. Cooper, "Spectrum Sensing in Interference and Noise Using Deep Learning," in *2020 54th Annual Conference on Information Sciences and Systems (CISS)*, Princeton, NJ, USA, 2020, pp. 1-6, doi: 10.1109/CISS48834.2020.1570617443.

[8] A. Nasser, H. Al H. Hassan, J. A. Chaaya, A. Mansour, and K.-C. Yao, "Spectrum sensing for cognitive radio: Recent advances and future challenge," *Sensors*, vol. 21, no. 7, pp. 1-29, 2021, doi: 10.3390/s21072408.

[9] T. Perarasi, G. Nagarajan, R. Gayathri, and M. L. Moses, "Evaluation of cooperative spectrum sensing with filtered bank multi carrier utilized for detecting in cognitive radio network," *Transactions on Emerging Telecommunications Technologies*, vol. 33, no. 7, 2022, doi: 10.1002/ett.4478.

[10] M. U. Muzaffar and R. Sharqi, "A review of spectrum sensing in modern cognitive radio networks," *Telecommunication Systems*, vol. 85, no. 2, pp. 347-363, 2024, doi: 10.1007/s11235-023-01079-1.

[11] S. Zheng, S. Chen, P. Qi, H. Zhou, and X. Yang, "Spectrum sensing based on deep learning classification for cognitive radios," *China Communications*, vol. 17, no. 2, pp. 138-148, Feb. 2020, doi: 10.23919/JCC.2020.02.012.

[12] J. Manco, I. Dayoub, A. Nafkha, M. Alibakhshikenari, and H. B. Thameur, "Spectrum sensing using software defined radio for cognitive radio networks: A survey," *IEEE Access*, vol. 10, pp. 131887–131908, 2022, doi: 10.1109/ACCESS.2022.3229739.

[13] I. Raghu and E. Elias, "Low complexity spectrum sensing technique for cognitive radio using Farrow structure digital filters," *Engineering Science and Technology, an International Journal*, vol. 22, no. 1, pp. 131-142, 2019, doi: 10.1016/j.jestch.2018.04.012.

[14] L. Li, M. V., R. S., E. G., and G. R. Gonzalez, "Metaheuristic FIR filter with game theory based compression technique-A reliable medical image compression technique for online applications," *Pattern Recognition Letters*, vol. 125, pp. 7-12, 2019, doi: 10.1016/j.patrec.2019.03.023.

[15] A. Sharma *et al*., "Recent trends in AI-based intelligent sensing," *Electronics*, vol. 11, no. 10, p. 1661, 2022, doi: 10.3390/electronics11101661.

[16] W. Ding, J. Shan, B. Fang, C. Wang, F. Sun, and X. Li, "Filter Bank Convolutional Neural Network for Short Time-Window Steady-State Visual Evoked Potential Classification," *IEEE Transactions on Neural Systems and Rehabilitation Engineering*, vol. 29, pp. 2615-2624, 2021, doi: 10.1109/TNSRE.2021.3132162.

[17] D. Xu, F. Tang, Y. Li, Q. Zhang, and X. Feng, "FB-CCNN: A filter bank complex spectrum convolutional neural network with artificial gradient descent optimization," *Brain Sciences*, vol. 13, no. 5, pp. 1-18, 2023, doi: 10.3390/brainsci13050780.

[18] J. Zhang, Z. -Q. He, H. Rui, and X. Xu, "Multiband Joint Spectrum Sensing via Covariance Matrix-Aware Convolutional Neural Network," *IEEE Communications Letters*, vol. 26, no. 7, pp. 1578-1582, July 2022, doi: 10.1109/LCOMM.2022.3163841.

[19] G. A. M. Novelo and G. J. Dolecek, "Spectrum Sensing with Filter Banks and Energy Detectors," in *13th International Conference on Mathematical Modeling in Physical Sciences*, 2025, vol. 3027, doi: 1742-6596/3027/1/012082.

[20] P. R A S Bassi and R. Attux, "FBDNN: Filter banks and deep neural networks for portable and fast brain-computer interfaces," *Biomedical Physics & Engineering Express*, vol. 8, 2022, doi: 10.1088/2057-1976/ac6300.

[21] A. Haldorai, J. Sivaraj, M. Nagabushanam, and M. K. Roberts, "Cognitive wireless networks based spectrum sensing strategies: A comparative analysis," *Applied Computational Intelligence and Soft Computing*, vol. 2022, 2022, doi: 10.1155/2022/6988847.

[22] M. Subbarao and N. V. Rao, "Modified parallel FFT energy detection using machine learning-based spectrum sensing," *Microsystem Technologies*, vol. 31, pp. 909–923, 2025, doi: 10.1007/s00542-024-05702-2.

[23] M. Y. Abdallah and D. M. Ali, "Evaluating the practical performance of energy detector-based spectrum sensing for cognitive radio," in *International Conference on Engineering and Advanced Technology: (ICEAT 2022)*, vol. 2787, no. 1, Jul. 2023, doi: 10.1063/5.0148461.

[24] S. Bagchi and J. Y. Siddiqui, "Spectrum sensing for cognitive radio using a filter bank approach," *Intelligent Multi-Modal Data Processing*, Eds. Wiley, ch. 9, 2021, doi: 10.1002/9781119571452.ch9.

[25] M. Sani, J. Tsado, S. Thomas, H. Suleiman, I. M. Shehu, and M. G. Shan'una, "A Survey on Spectrum Sensing Techniques for Cognitive Radio Networks," in *2021 1st International Conference on Multidisciplinary Engineering and Applied Science (ICMEAS)*, Abuja, Nigeria, 2021, pp. 1-5, doi: 10.1109/ICMEAS52683.2021.9692412.

[26] R. R. Yakkati, R. R. Yakkati, R. K. Tripathy and L. R. Cenkeramaddi, "Radio Frequency Spectrum Sensing by Automatic Modulation Classification in Cognitive Radio System Using Multiscale Deep CNN," *IEEE Sensors Journal*, vol. 22, no. 1, pp. 926-938, 2022, doi: 10.1109/JSEN.2021.3128395.

[27] A. K. Parvathi and S. Vellaisamy, "Low complexity adaptive spectrum sensing using modified frm filter bank," *International Journal of Electronics*, vol. 109, no. 12, pp. 2015-2034, 2022, doi: 10.1080/00207217.2021.2001866.

[28] P. Y. Dibal, E. Onwuka, C. Alenoghena, and J. Agajo, "Discrete wavelet packet based spectrum sensing in cognitive radio using an improved adaptive threshold," in *Proceedings of the International Conference on Industrial Engineering and Operations Management* Bandung, Indonesia, 2018, pp. 1723-1734.

[29] O. Serghini, H. Semlali, A. Maali, A. Ghammaz, and S. Serrano, "1-D convolutional neural network-based models for cooperative spectrum sensing," *Future Internet*, vol. 16, no. 1, p. 14, 2023, doi: 10.3390/fi16010014.

[30] W. El-Shafai, A. Fawzi, A. Sedik, A. Zekry, G. M. El-Banby, A. A. Khalaf, and M. Abd-Elnaby, "Convolutional neural network model for spectrum sensing in cognitive radio systems," *International Journal of Communication Systems*, vol. 35, no. 6, p. e5072, 2022, doi: 10.1002/dac.5072.

[31] N. Dewangan, A. Kumar, and R. N. Patel, "Performance Analysis of LSTM-CNN for Spectrum Sensing in Cognitive Radio Networks," *Mathematical Statistician and Engineering Applications*, vol. 71, no. 4, pp. 6218–6229, 2022, doi: 10.17762/msea.v71i4.1217.

BIOGRAPHIES OF AUTHORS

Hamza Ouamna is an electrical engineer and Ph.D. candidate specializing in spectrum sensing for vehicular environments. He received his Master of Engineering degree in Electrical Engineering and Control of Industrial Systems from ENSET Mohammedia, Hassan II University Casablanca. Currently, he is conducting research in Advanced Systems Engineering Laboratory (ISA), National School of Applied Sciences (ENSAK), Ibn Tofail University Kenitra. His research aims to develop efficient and robust spectrum sensing techniques for vehicular communications. He can be contacted at email: hamza.ouamna@uit.ac.ma.

Noureddine El-Haryqy is a researcher who graduated in 2021 with a master's degree in embedded electronics from the Faculty of Science at Ibn Tofail University in Kenitra, Morocco. His Ph.D. research is focused on the application of artificial intelligence for dynamic spectrum management. Located in the Department of Electrical and Telecommunications at the National School of Applied Sciences, Ibn Tofail University, Kenitra, Morocco. He can be contacted at email: noureddine.elharyqy@uit.ac.ma.

Anass Kharbouche received his Master's degree in embedded systems and telecommunication systems in 2018. He continued his studies as a doctoral student (Ph.D.) in the Advanced Systems Engineering Laboratory (ISA) research group at the National School of Applied Sciences (ENSAK), Ibn Tofail University, Kenitra, Morocco. He obtained his Ph.D. in Electrical Engineering and Telecommunications in 2024. His research interests include optoelectronic devices, fiber optic communications, free-space optical communications, artificial intelligence, spectrum sensing, cognitive radio, signal processing, and V2X communications. He can be contacted at email: anass.kharbouche@uit.ac.ma.

Zhour Madini received her Master of Engineering degree from the Optical and Microwave Communications Research Institute, Limoges France. She received her Ph.D. degree from University of Limoges in High Frequency Telecommunications and Optic in 2008. She is now a higher education professor in Electronics and Telecommunications at National School of Applied Sciences of Kenitra (ENSAK). Her current research interests include electronic devices, digital signal processing for communications, fiber-optic communication systems, and cognitive radio technology. She can be contacted at email: zhour.madini@uit.ac.ma.

Younes Zouine received his Master of Engineering degree from the National School of Engineers of Limoges (ENSIL) in 2002. He received his Ph.D. in High Frequency Telecommunications and Optics from the University of Limoges in 2005. He joined the National School of Applied Sciences of kenitra (ENSAK), Ibn Tofail University, as Professor of Electronics and Telecommunications. His current research interests deal with digital signal processing for communications and especially with theory and implementation of signal processing for optical systems. He can be contacted at email: younes.zouine@uit.ac.ma.